Theoretical Investigations of the Electrochemical Reduction of CO on Single Metal Atoms Embedded in Graphene

Charlotte Kirk,[1],[2],[†] Leanne D. Chen,[2],[3],[†] Samira Siahrostami,[1],[†] Mohammadreza Karamad,[1] Michal Bajdich,[2] Johannes Voss, [2] Jens K. Nørskov,[1],[2] Karen Chan[2]*

[1] SUNCAT Center for Interface Science and Catalysis, Department of Chemical Engineering, Stanford University, 443 Via Ortega, Stanford, California 94305, United States

[2] SUNCAT Center for Interface Science and Catalysis, SLAC National Accelerator Laboratory, 2575 Sand Hill Road, Menlo Park, California 94025, United States

[3] Division of Chemistry and Chemical Engineering, California Institute of Technology, Pasadena, CA 91125

[†]Contributed equally

*email: chank@stanford.edu

Supplementary Note 1: Benchmarking Magnetic Moments

All calculations were performed with spin polarization. We applied the model developed by Krasheninnikov et al.[1] as an initial guess for the spin state of the metal atom in a graphene single vacancy. We do not see a large impact of the spin state of the metal atom on adsorption energies. We obtained less than 0.1 eV variation between calculations with the appropriate magnetic moments and calculations with all magnetic moments set equal to 0, as illustrated in Supplementary Figure 1.

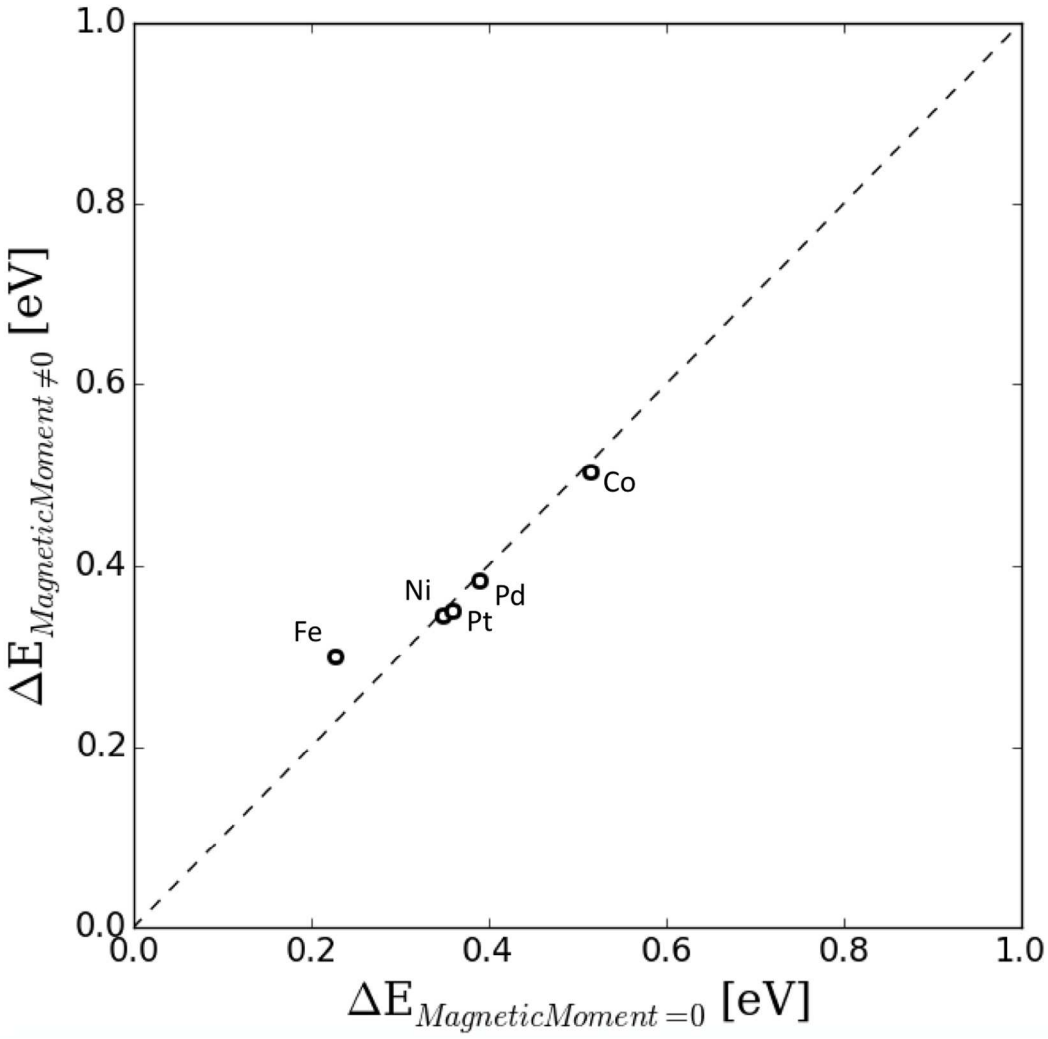

Supplementary Figure 1: Parity plot of the electronic reaction energy for the reaction $* CO + H^+ + e^- \leftrightarrow * CHO$ on M@SV surfaces. On the x axis, all magnetic moments of the metal atom are equal to zero. On the y axis, specified magnetic moments follow the scheme proposed by Krasheninnikov et al.[1] Magnetic moments are given in Supplementary Table 1.

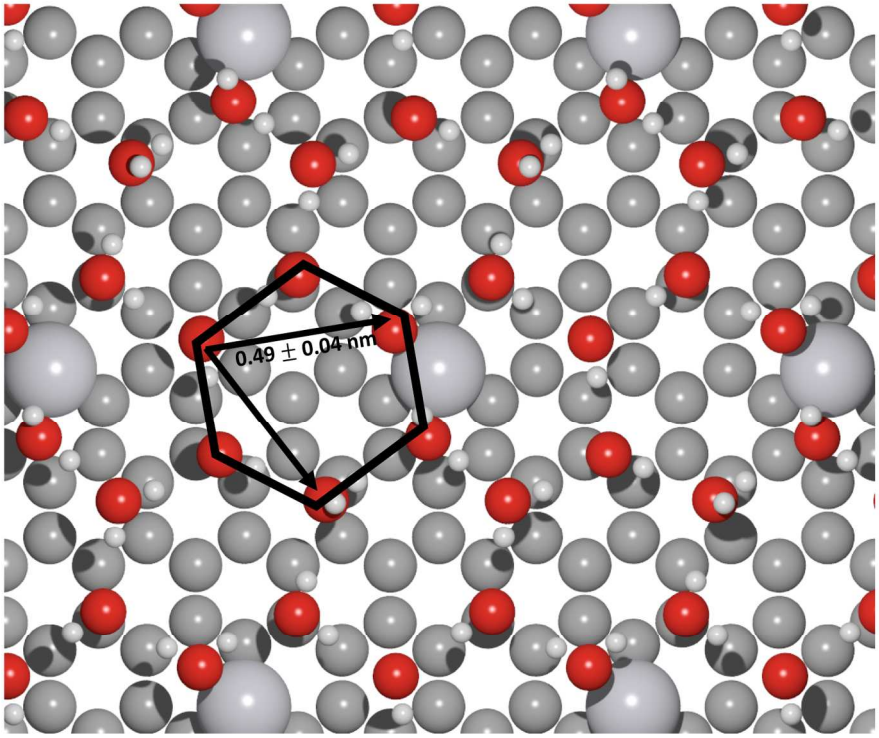

Supplementary Figure 2: Water structure of bare surface determined through minima hopping. The short diameter of the hexagon was found to be 0.49 ± 0.04 nm, which is very close to values previously determined computationally and experimentally for non-doped graphene.[2,3]

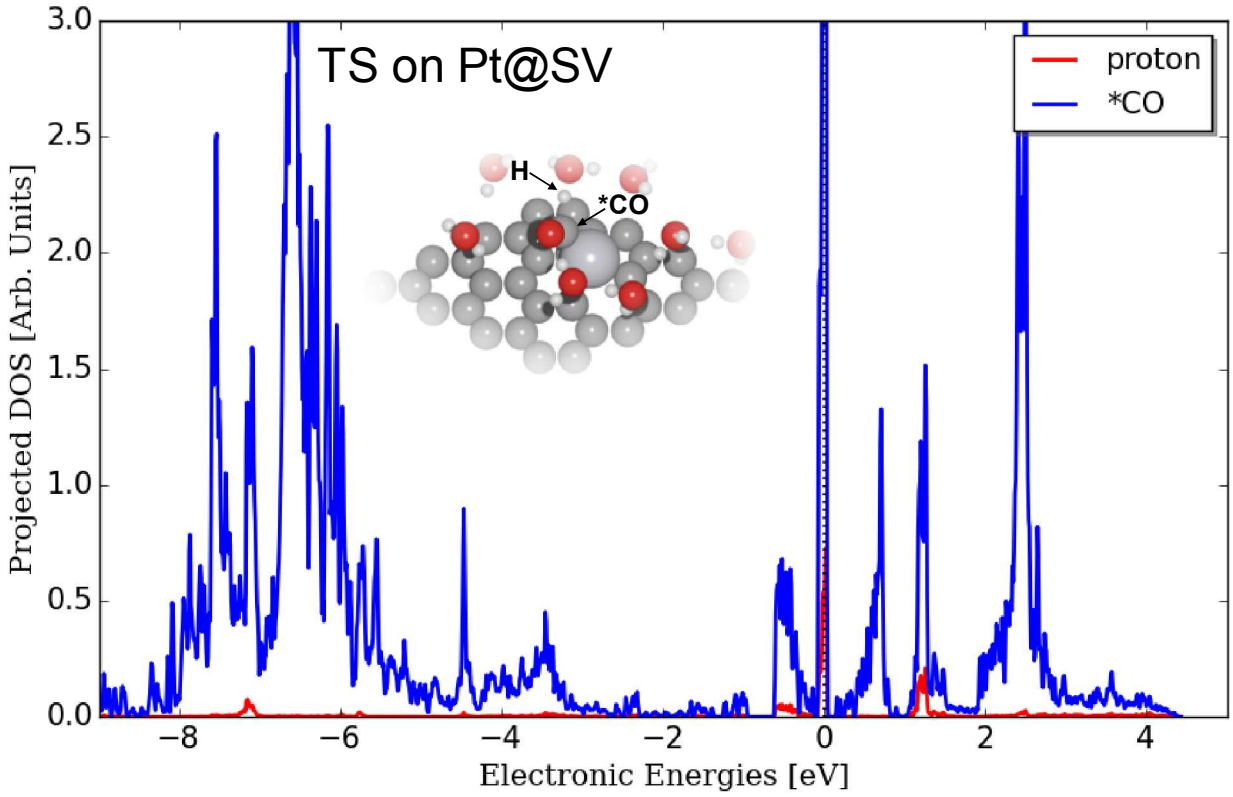

Supplementary Figure 3: Projected density of states of the s and p orbitals on adsorbed CO and s orbital of the proton in the transition state for the reaction *CO + H^+/e^- → *CHO on Pt@SV computed using a smearing of 0.01eV and k-point sampling of (16x16x1).The width of the peak at the Fermi level is on the order of 0.1 eV, corresponding to an electron lifetime on the order of 10^{-14} s via the Heisenberg uncertainty principle.

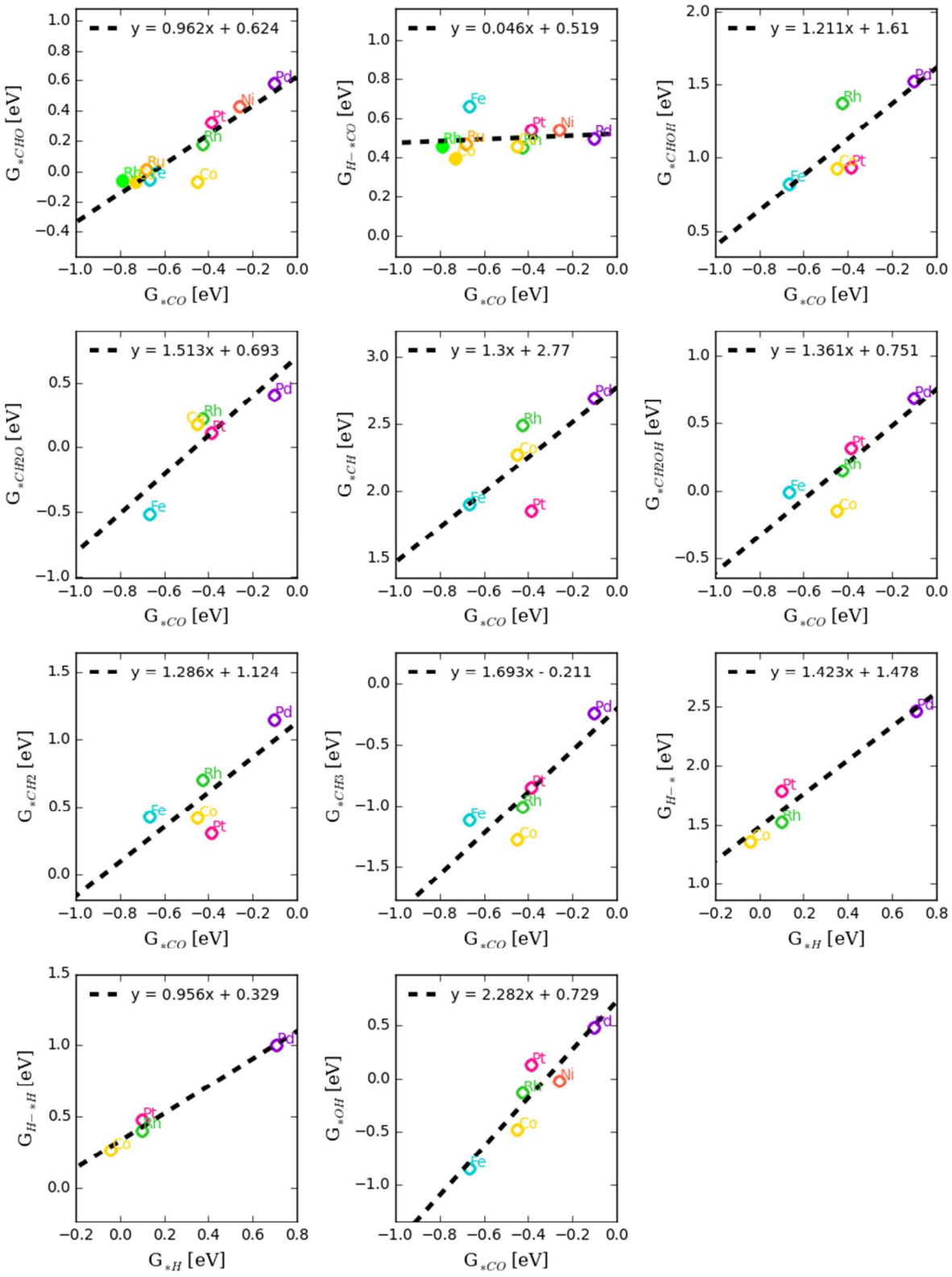

Supplementary Figure 4: Scaling relations of intermediate binding energies and transition state energies used in kinetic model.

a) b)

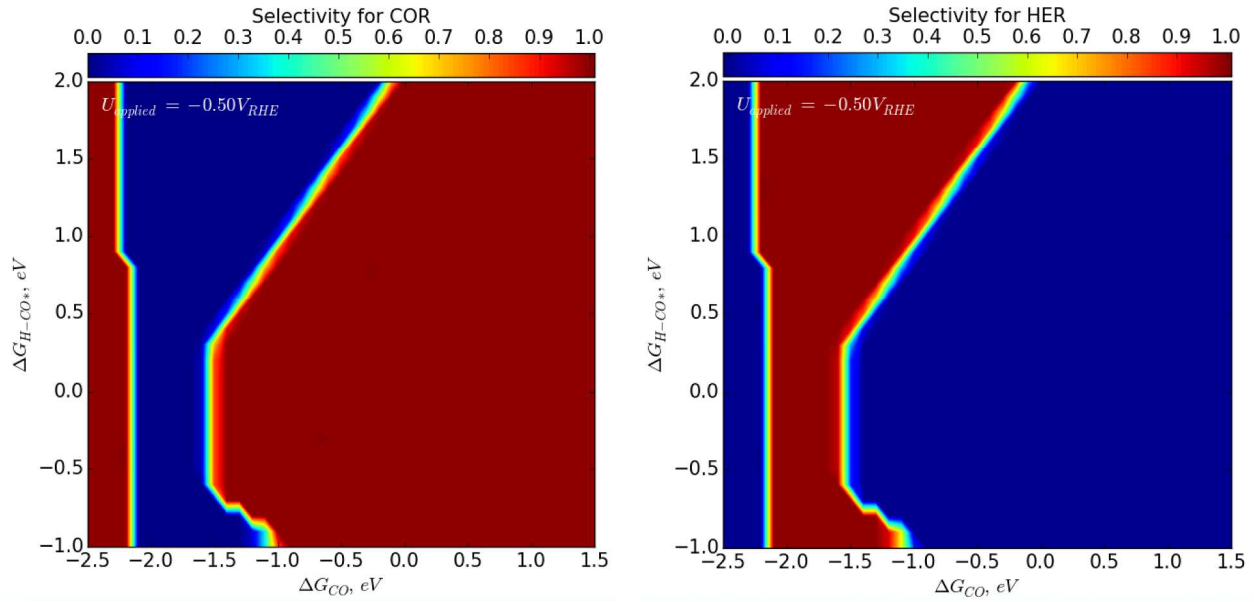

Supplementary Figure 5: Selectivity for the CO reduction reaction (a) and hydrogen evolution (b) reaction at -0.5 V_{RHE}.

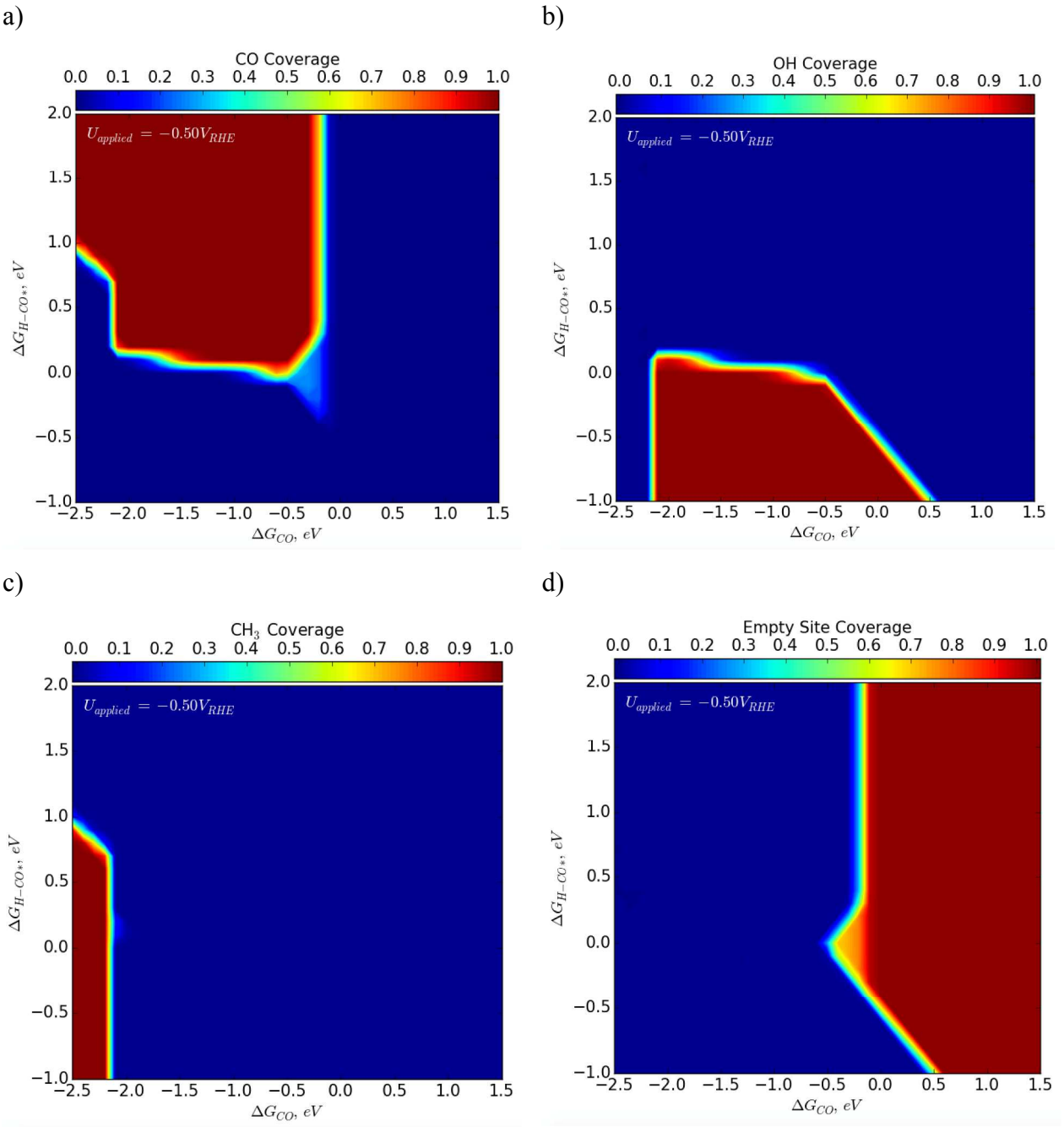

Supplementary Figure 6: Surface coverage of CO (a), OH (b), CH_3 (c), and empty sites (d) at -0.5 V_{RHE}. All other coverages were found to be near 0.

Supplementary Table 1: Magnetic moments of the metal atom in the M@SV surface following the work of Krasheninnikov et al.[1] The magnetic moments for the metal atom in a bare surface, with CO adsorbed, and with CHO adsorbed are given.

M@SV	Bare Surface	*CO	*CHO
Ni	0	0	1
Pd	0	0	1
Pt	0	0	1
Co	1	1	0
Rh	1	1	0
Fe	0	0	1
Ru	0	0	1

Supplementary table 2: Energies of formation of M@SV with respect to bulk chemical as shown in Figure 1a.

M@SV	Formation Energy [eV]
Cu	-0.53
Ni	-2.33
Pd	-1.84
Pt	-2.07
Co	-2.91
Rh	-2.88
Ir	-2.41
Fe	-1.99
Ru	-2.14
Os	-1.67
Cr	-2.72
Mo	-1.55
W	-0.72

Supplementary table 3: Free energies of intermediates and barriers for the reduction path of $CO_{(g)}$ to $CH_{4\,(g)}$ on Pt@SV at 0 V_{RHE} and -0.5 V_{RHE} as shows in Figure 1.

Reaction	ΔG_A, 0V_{RHE} [eV]	ΔG_A -0.5V_{RHE} [eV]
$*CO + H^+ + e^- \rightarrow *CHO$	0.93	0.64
$*CHO + H^+ + e^- \rightarrow *CHOH$	0.58	0.18
$*CHO + H^+ + e^- \rightarrow *CH_2O$	0.67	0.27
$*CH_2O + H^+ + e^- \rightarrow *CH_2OH$	0.74	0.32
$*CH + H^+ + e^- \rightarrow *CH_2$	-0.11	-0.48
$*CH_2OH + H^+ + e^- \rightarrow *CH_2 + H_2O_{(g)}$	0.42	0.31
$*CH_2 + H^+ + e^- \rightarrow *CH_3$	0.02	-0.22
$*CH_3 + H^+ + e^- \rightarrow CH_{4\,(g)}$	0.47	0.17

Supplementary Table 4: Activation energies for the reactions

$$* CO + H^+ + e^- \leftrightarrow * CHO \quad (1)$$

$$* + H^+ + e^- \leftrightarrow * H \quad (2)$$

$$* H + H^+ + e^- \leftrightarrow * + H_{2\,(g)} \quad (3)$$

vs. the *CO binding energy for M@SV surfaces at 0 V vs. RHE as shown in main text Figure 1a and Figure 4b.

M@SV	ΔG_{*CO} [eV]	ΔG_A [eV] (1)	ΔG_A [eV] (2)	ΔG_A [eV] (3)
Pt	-0.39	0.92	1.70	0.38
Pd	-0.10	0.60	1.76	0.29
Co	-0.45	0.91	1.40	0.30
Rh	-0.43	0.88	1.42	0.31
Fe	-0.67	1.33	/	/
Ru	-0.68	1.15	/	/
Ni	-0.26	0.80	/	/
Rh (N dopant)	-0.79	1.25	/	/
Co (N dopant)	-0.73	1.12	/	/

Supplementary Table 5: Binding energies of intermediates used in finding scaling relations for kinetics. Scaling relations are shown in Supplementary Figure 4.

ΔG_{ads}									
M@SV	*CO	*CHO	*CH_2O	*CH_2OH	*CH_2	*CH_3	*CHOH	*CH	*COH
Pt	-0.39	0.32	0.11	0.32	0.31	-0.85	0.94	1.85	2.05
Pd	-0.10	0.58	0.40	0.69	1.15	-0.24	1.52	2.69	2.61
Co	-0.45	-0.06	0.17	-0.15	0.42	-1.28	0.93	2.27	1.91
Rh	-0.43	0.18	0.22	0.15	0.70	-1.01	1.37	2.49	/
Fe	-0.67	-0.055	-0.51	-0.013	0.43	-1.12	0.83	1.90	/

(1) Krasheninnikov, A. V.; Lehtinen, P. O.; Foster, A. S.; Pyykkö, P.; Nieminen, R. M. Embedding transition-metal atoms in graphene: Structure, bonding, and magnetism. *Phys. Rev. Lett.* **2009**, *102* (12), 126807.

(2) Kimmel, G. A.; Matthiesen, J.; Baer, M.; Mundy, C. J.; Petrik, N. G.; Smith, R. S.; Dohnálek, Z.; Kay, B. D. No confinement needed: Observation of a metastable hydrophobic wetting two-layer ice on graphene. *J. Am. Chem. Soc.* **2009**, *131* (35), 12838.

(3) Teschke, O. Imaging ice-like structures formed on HOPG at room temperature. *Langmuir* **2010**, *26* (22), 16986.